

Light-shift-induced photonic nonlinearities

This content has been downloaded from IOPscience. Please scroll down to see the full text.

2008 New J. Phys. 10 043010

(<http://iopscience.iop.org/1367-2630/10/4/043010>)

View [the table of contents for this issue](#), or go to the [journal homepage](#) for more

Download details:

IP Address: 131.215.193.135

This content was downloaded on 24/05/2016 at 00:14

Please note that [terms and conditions apply](#).

Light-shift-induced photonic nonlinearities

F G S L Brandão^{1,2,3}, M J Hartmann^{1,2} and M B Plenio^{1,2}

¹ Institute for Mathematical Sciences, Imperial College London,
53 Exhibition Road, SW7 2PE, UK

² QOLS, The Blackett Laboratory, Imperial College London,
Prince Consort Road, SW7 2BW, UK

E-mail: fernando.brandao@imperial.ac.uk

New Journal of Physics **10** (2008) 043010 (14pp)

Received 4 October 2007

Published 10 April 2008

Online at <http://www.njp.org/>

doi:10.1088/1367-2630/10/4/043010

Abstract. We propose a new method to produce self- and cross-Kerr photonic nonlinearities, using light-induced Stark shifts due to the interaction of a cavity mode with atoms. The proposed experimental set-up is simpler than in previous approaches, while the strength of the nonlinearity obtained with a single atom is the same as in the setting based on electromagnetically induced transparency. Furthermore our scheme can be applied to engineer effective photonic nonlinear interactions whose strength increases with the number of atoms coupled to the cavity mode, leading to photon–photon interactions several orders of magnitude larger than previously considered possible.

³ Author to whom any correspondence should be addressed.

Contents

1. Introduction	2
2. Derivation of the effective model	3
2.1. Dispersive regime nonlinearity	4
2.2. Extra driving laser field	4
2.3. Stark-shift nonlinearity	4
3. Many atoms regime	6
4. Error analysis and numerics	7
5. Cross-Kerr nonlinearities	9
6. Possible experimental realizations	10
7. Summary	11
Acknowledgments	11
Appendix. Derivation of the effective dynamics	11
References	13

1. Introduction

Quantum properties of light, such as photon anti-bunching [1] and photonic entanglement [2], can only be produced by nonlinear interactions between photons. Strong nonlinearities are also important for quantum information processing, with applications ranging from quantum nondemolition measurements [3] to quantum memories for light [4] and optical quantum computing architectures [5]. However, photon–photon interactions are usually extremely weak, and several orders of magnitude smaller than those needed in the above applications. A possible route towards larger nonlinearities is the use of coherent interaction between light and matter in high finesse quantum electrodynamics (QED) cavities [6]. The goal here is to produce large nonlinearities with negligible losses, something which cannot be accomplished by merely tuning atom–light interactions close to resonance. To the best of our knowledge, the setting generating the largest nonlinear interactions in this context, proposed by Imamoglu and co-workers [7]–[9], uses quantum interference effects related to electromagnetically induced transparency (EIT) [10] to produce giant Kerr nonlinearities. These nonlinearities were shown to be essentially absorption free and up to 9 orders of magnitude larger than natural Kerr interactions (see figure 1(a))⁴ (see e.g. [11, 12] for related experimental implementations). Another distinctive feature of this scheme is that the ratio nonlinearity strength over losses can be kept constant when several atoms interact with the same cavity mode.

Here we propose a new method for producing Kerr nonlinearities in cavity QED systems which is (i) experimentally less demanding, requiring one atomic level and one coupling to the cavity mode less than in the EIT setting, (ii) virtually absorption free, and (iii) produces nonlinearities comparable or even superior to the state-of-art EIT scheme [7]. By applying suitable laser pulses at the beginning and end of the evolution of the proposed set-up, we obtain nonlinear interactions whose (iv) strength increases with increasing number of atoms interacting

⁴ As shown in [8], the EIT setting can produce nonlinearities with a strength of $\alpha\beta g$, where g is the Rabi frequency of the atom–cavity interaction and α, β are two parameters which must be much smaller than one.

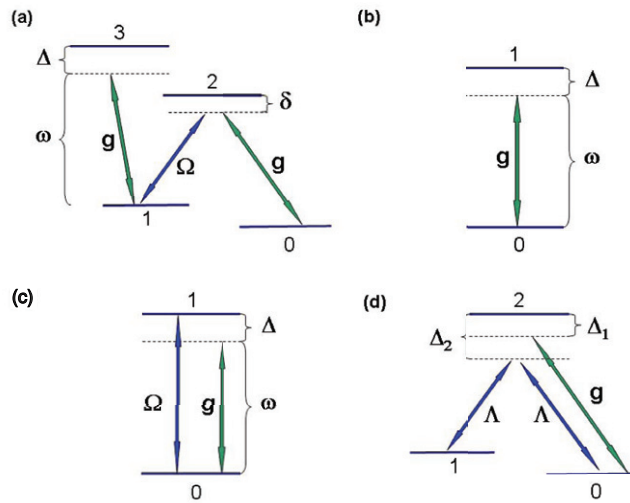


Figure 1. (a) EIT scheme considered in [7, 8], (b) dispersive regime of the Jaynes–Cummings interaction, (c) large but noisy nonlinearity scheme and (d) scheme proposed in this paper. Coupling to the cavity mode is shown in green and to classical lasers in blue.

with the cavity mode, leading to effective nonlinear interactions at least two orders of magnitude larger than previously considered possible⁵. This brings closer to reality a number of proposals for quantum computation and communication based on photonic nonlinearities as well as the observation of many-body phenomena in systems consisting of arrays of coupled cavities [8, 9], [13]–[19] where quantum-phase transitions for polaritons and photons [9], [13]–[15], as well as a photonic Mott-insulator [8]—in which photons would be frozen inside each cavity—could be observed experimentally provided strong photonic nonlinearities are available. The estimated strength of our nonlinearity would also suffice for the implementation of quantum nondemolition measurements [20], a photonic CNOT gate [21], and continuous variable entanglement distillation [22]. We discuss several possible experimental settings [12], [23]–[30] and typical as well as predicted parameters in such systems at the end of this paper.

In our approach, the relevant atomic level structure, depicted in figure 1(d), is a Λ system with two metastable states and an excited state. The cavity mode couples dispersively only to the 0–2 transition and the levels 0 and 1 are coupled via a far-detuned Raman transition. Finally, the detuning associated with the lasers and with the cavity mode are assumed to be very different from each other.

2. Derivation of the effective model

In this section, we show how the effective photonic nonlinearity can be obtained from the set-up proposed above. In order to gain intuitive understanding why our model works, we first present

⁵ We note that our figure of merit when comparing one to several atoms schemes is that the total population in the excited state is kept the same. Therefore we say that more atoms produce a larger nonlinearity in comparison when, while maintaining the same decoherence rate due to spontaneous emission, the strength of the effective nonlinearity increases with the number of atoms coupled to the cavity mode.

two simple schemes to engineer nonlinearities and discuss their drawbacks. We then turn to the new set-up we propose and show how it overcomes the limitations of the previous ones.

2.1. Dispersive regime nonlinearity

To understand intuitively how our scheme works, let us start with the simplest system producing a nonlinearity: N two level atoms interacting dispersively with a cavity mode a (see figure 1(b)). The system can be described by the Jaynes–Cummings Hamiltonian, which in the interaction picture with respect to $H_0 = \omega a^\dagger a + \omega_0 \sum_k |1_k\rangle\langle 1_k|$ reads

$$H = g(e^{-i\Delta t} a S_{10} + e^{i\Delta t} a S_{01}), \quad (1)$$

where $S_{10} := \sum_k |1_k\rangle\langle 0_k|$, g is the Rabi frequency of the Jaynes–Cummings interaction, and Δ the detuning of the cavity mode frequency to the atomic transition frequency. If $\sqrt{N}g/\Delta \ll 1$, the system is in the so-called dispersive regime and we can adiabatically eliminate the upper level, as its population is negligible. Including fourth order terms in the perturbation theory and neglecting nonenergy preserving terms, we can approximate the Hamiltonian above as

$$H_{\text{eff}}^{(1)} = \frac{Ng^2}{\Delta} a^\dagger a (S_{00} - S_{11}) + \frac{Ng^4}{\Delta^3} a^\dagger a a^\dagger a (S_{00} - S_{11}), \quad (2)$$

where $S_{aa} := \sum_{k=1}^N |a_k\rangle\langle a_k|$. Hence, if all atoms are prepared in their ground states, we obtain a self Kerr nonlinearity $\chi = Ng^4/\Delta^3$. This scheme has two major drawbacks. Firstly, the obtained nonlinearities are at least one order of magnitude smaller than in the EIT setting. Secondly, because of $\sqrt{N}g/\Delta \ll 1$, characterizing the dispersive regime, the nonlinearity decreases as g/\sqrt{N} .

2.2. Extra driving laser field

A simple solution to both these problems is to add a classical laser in resonance to the transition $|0\rangle \rightarrow |1\rangle$ (see figure 1(c)). Under the conditions $\sqrt{N}g/\Delta \ll 1$ and $\sqrt{N}g^2/\Delta \ll \Omega$, the dynamics of the system is well described by

$$H_{\text{eff}}^{(2)} = \frac{Ng^2}{\Delta} a^\dagger a S_3 + \frac{\sqrt{N}g}{\Delta} \frac{\sqrt{N}g^2}{\Delta\Omega} g a^\dagger a a^\dagger a S_3, \quad (3)$$

where $S_3 := \sum_{k=1}^N |+_k\rangle\langle +_k| - |-_k\rangle\langle -_k|$, with $|\pm\rangle = (|0\rangle \pm |1\rangle)/\sqrt{2}$. Hence, preparing the atomic states in the superposition $|- \rangle$, we find a nonlinearity as large as in the EIT setting which does not decrease with the number of atoms. Unfortunately, this improvement comes at the price of a large increase in the losses due to spontaneous emission which will destroy the atomic superpositions, quickly decreasing the effective nonlinearity.

2.3. Stark-shift nonlinearity

In our proposed scheme (see figure 1(d)), we have a situation similar to the one discussed above. Indeed, the effective Hamiltonian will be identical to $H_{\text{eff}}^{(2)}$. However, now the states $|\pm\rangle$ are metastable, which makes the system almost decoherence free. The full Hamiltonian of the system, in the interaction picture with respect to $H_0 = \omega a^\dagger a + \omega_1 \sum_k |1_k\rangle\langle 1_k|$ reads:

$$H = g(e^{-i\Delta_1 t} a S_{20} + e^{i\Delta_1 t} a^\dagger S_{02}) + \sqrt{2}\Lambda(e^{-i\Delta_2 t} S_{2+} + e^{-i\Delta_2 t} S_{+2}), \quad (4)$$

where $S_{20} := \sum_k |2_k\rangle\langle 0_k|$ and $S_{2+} := \sum_k |2_k\rangle\langle +_k|$. We assume for the moment that all the atoms interact in the same manner with the cavity mode. As shown in figure 1(d), (g, Δ_1) and (Λ, Δ_2) are the Rabi frequencies and detunings of the cavity–atom and laser–atom interactions, respectively. To justify the use of the single mode paradigm we require that $\Delta_1, \Delta_2 \gg \kappa$, where κ is the cavity decay rate. We are interested in the dispersive regime, characterized by:

$$\frac{\sqrt{N}g}{\Delta_1} \ll 1, \quad \frac{\sqrt{N}\Lambda}{\Delta_2} \ll 1. \quad (5)$$

Moreover, we assume that

$$\sqrt{N}g, \sqrt{N}\Lambda \ll |\Delta_2 - \Delta_1|, \quad (6)$$

so that we can treat the processes driven by the cavity–atom and laser–atom interactions independently. Under these conditions the dynamics of the system will be described by the one of a self-Kerr photonic nonlinearity. In the sequel we outline the main steps taken to derive the effective Hamiltonian for the model. A more in-depth analysis is given in the appendix.

Under the above conditions the excited state will hardly be populated, and we can adiabatically eliminate it, finding an effective Hamiltonian for the two metastable states and the cavity mode. In turn, these will experience ac Stark shifts due to the interaction with the upper level. The effective Hamiltonian, dropping out terms proportional to the identity, is given by

$$H_1 = \frac{g^2}{\Delta_1} a^\dagger a S_{00} + \frac{\Theta}{2} (S_{10} + S_{01}), \quad (7)$$

with $\Theta := 2\Lambda^2/\Delta_2$. If we now go to a second interaction picture with respect to $H_0 = (g^2/2\Delta_1) a^\dagger a$ we find

$$H_1^{\text{int}} = \frac{g^2}{2\Delta_1} a^\dagger a (S_{+-} + S_{-+}) + \frac{\Theta}{2} S_3, \quad (8)$$

where $S_{+-} := \sum_k |+_k\rangle\langle -_k|$, $S_{-+} = (S_{+-})^\dagger$, and, as before, $S_3 := \sum_{k=1}^N |+_k\rangle\langle +_k| - |-_k\rangle\langle -_k|$. It follows that in the $\{| \pm \rangle\}$ basis the system can be viewed as an ensemble of two level atoms driven by a laser with a photon-number-dependent Rabi frequency. If we consider the dispersive regime of this system, i.e.

$$\frac{\sqrt{N}g^2}{2\Delta_1\Theta} \ll 1, \quad (9)$$

the atoms prepared in the $|-\rangle$ state will experience a Stark shift proportional to $(a^\dagger a)^2$, which gives rise to the desired Kerr nonlinearity. The effective Hamiltonian will be given by $H_{\text{eff}} = (g^4/4\Delta_1^2\Theta) a^\dagger a a^\dagger a S_3$. Therefore, if we prepare all the atomic states in the $|-\rangle$ state, one obtains an essentially absorption free Kerr nonlinearity given by

$$H_{\text{kerr}} = \underbrace{\frac{\sqrt{N}g^2}{2\Delta_1\Theta}}_{\ll 1} \underbrace{\frac{\sqrt{N}g}{2\Delta_1}}_{\ll 1} g a^\dagger a a^\dagger a. \quad (10)$$

In the regime we consider, characterized by equations (5) and (9), the first two terms $(\sqrt{N}g^2/2\Delta_1\Theta)$ and $(\sqrt{N}g/2\Delta_1)$ must be much smaller than one. We can also see that the strength of the effective Kerr nonlinearity does not depend on the number of atoms, as we can tune Δ_1 and Θ independently. As such, the maximum achievable nonlinearity is limited by g ,

which depends on the properties of the cavity and of the atoms employed. A more detailed derivation of effective Hamiltonian given by equation (10) is presented in the appendix.

We note that under the conditions we impose each atom interacts independently with the cavity mode. Therefore, if each atom has a different Rabi frequency g_i , which is the case when e.g. an atomic cloud is released in an optical cavity, then the resulting nonlinear coupling term will be identical to the one given by equation (10), but with g^4 replaced by $\sum_i g_i^4$. Moreover, for the same reason the scheme is robust if some of the atoms are not in the $|-\rangle$ state, which is clear from the form of H_{eff} .

3. Many atoms regime

We now proceed to show that, in fact, our set-up can be modified to give nonlinear interactions which increase with N . The joint atomic operators S_{+-} , S_{-+} and S_3 satisfy $su(2)$ commutation relations:

$$[S_{+-}, S_{-+}] = S_3, \quad [S_3, S_{\pm\mp}] = \pm S_{\pm\mp}. \quad (11)$$

Defining the canonical transformation $U = \exp(\mu a^\dagger a (S_{+-} - S_{-+}))$, with $\mu := g^2/(\Delta_1 \Theta) \ll 1$ [31], we can use the Hausdorff expansion ($\exp(xA)B\exp(-xA) = B + x[A, B] + x^2[A, [A, B]]/2 + \dots$) to obtain from equation (8)

$$H_{\text{rot}} := U^\dagger (H_1^{\text{int}}) U \approx \frac{\Theta}{2} S_3 - \left(\frac{g^2}{2\Delta_1} \right)^2 \frac{1}{\Theta} (a^\dagger a)^2 S_3 + \left(\frac{g^2}{2\Delta_1} \right)^3 \frac{1}{\Theta^2} (a^\dagger a)^3 (S_{+-} + S_{-+}). \quad (12)$$

Suppose we had a way of generating H_{rot} . If we prepared all the atoms in the $|-\rangle$ state, the effective photonic Hamiltonian would be given by the second term in equation (12) as long as

$$\left(\frac{g^2}{2\Delta_1} \right)^3 \frac{\sqrt{N}}{\Theta^3} \ll 1. \quad (13)$$

The condition above is given by the ratio of the coefficient of the normalized atomic operator S_3/\sqrt{N} , given by $(\sqrt{N}\Theta/2)$, and the coefficient of the term $(a^\dagger a)^3 (S_{+-} + S_{-+})$, equal to $(g^2/2\Delta_1)^2 \frac{1}{\Theta}$. The former gives the energy spacing between the first and second collective atomic excitation in the rotated basis, whereas the later is responsible for Rabi oscillations between these. Condition (13) then ensures that basically no transition from $|-\rangle$ to $|+\rangle$ happens. Note that it is much less stringent than the one given by equation (9). In particular, setting Θ such that $(g^2/2\Delta_1)/\Theta = N^{-1/4}$, equation (13) is satisfied for large N , and we obtain a nonlinearity of

$$(\sqrt{N}g/\Delta_1)N^{1/4}ga^\dagger aa^\dagger a, \quad (14)$$

while maintaining the same level of error due to spontaneous emission, dephasing and cavity decay rate. For instance, with $N = 10^4$ and $(\sqrt{N}g/\Delta_1) = 0.1$, we obtain a nonlinearity equal to the Rabi frequency g , which is at least two orders of magnitude larger than possible in the single atom case.

It is indeed possible to realize the unitary operator $V(t) = \exp(itH_{\text{rot}})$ for every t . We have that $V(t) := U^\dagger \exp(itH_1^{\text{int}})U$, hence it suffices to show how to create the unitary U . Consider the Hamiltonian given by equation (4) when the classical lasers are switched off,

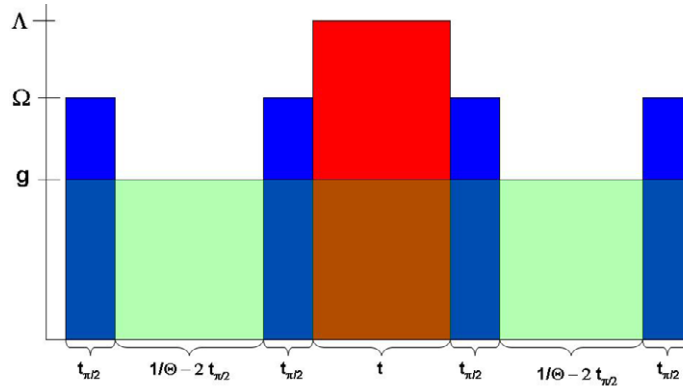


Figure 2. Sequence of operations generating $V(t)$. Blue and red areas correspond to the time the lasers with Rabi frequencies Ω and Λ are on, respectively. The green area illustrates that the Jaynes–Cummings interaction between the cavity mode and the atoms is on at all times. The scales do not reproduce reality in general. For example, t will be much larger than $1/\Theta$ in most cases.

i.e. $H = g(e^{-i\Delta_1 t} a S_{20} + e^{i\Delta_1 t} a^\dagger S_{02})$. Suppose we apply to the atoms a fast laser pulse, described by the unitary operator M that generates the transformation

$$|0_k\rangle \rightarrow (|0_k\rangle + i|1_k\rangle)/\sqrt{2}, \quad |1_k\rangle \rightarrow (|0_k\rangle - i|1_k\rangle)/\sqrt{2}, \quad (15)$$

let Hamiltonian H run for a time t and apply the inverse transformation M^\dagger . Then, the total evolution operator will be given by

$$\begin{aligned} M^\dagger \exp \left(ig \int_0^t (e^{-i\Delta_1 t'} a S_{20} + e^{i\Delta_1 t'} a^\dagger S_{02}) dt' \right) M \\ = \exp \left(ig \int_0^t \sqrt{2} g (e^{-i\Delta_1 t'} a (S_{20} + iS_{21}) + \text{h.c.}) dt' \right). \end{aligned} \quad (16)$$

As $\sqrt{N}g/\Delta_1 \ll 1$, we can once more adiabatically eliminate level 2 and approximate the unitary evolution above by $\exp(t(g^2/\Delta_1)a^\dagger a(S_+ - S_-))$, which is U when $t = 1/\Theta$. The sequence of operations executing $V(t)$ is shown in figure 2.

4. Error analysis and numerics

In order to check the accuracy of our approach, we simulated it numerically for one and two atoms. We assume that the unitary evolution given by equation (16) is created by a $\pi/2$ pulse of the Hamiltonian $H_{\text{laser}} = \Omega(|0\rangle\langle 1| + |1\rangle\langle 0|)$. We choose $\Omega = 100g$, which gives a $t_{\pi/2} = \pi/(2\Omega)$. The other parameters are $g = 10^8 \text{ s}^{-1}$, $5\Theta = gN^{1/3}$, and $\Delta_1 = 10\sqrt{N}g$. With these values, the quality of the approximation, which is determined by the value of the LHS of equation (13) and $\sqrt{N}g/\Delta_1$, should be constant. A good figure of merit in this respect is given by $X = |\langle n| \otimes \langle -| V(t) | - \rangle \otimes | n \rangle|$, where $V(t)$ is the total unitary operator formed by concatenating the steps explained above (see figure 2 for a graphic description of the procedure), $|n\rangle$ is the n th Fock state of the photons, and $|-\rangle := |-\rangle_1 \otimes \cdots \otimes |-\rangle_N$. In the case of an ideal Kerr nonlinearity X should be equal to one at all instants of time. As can be seen in

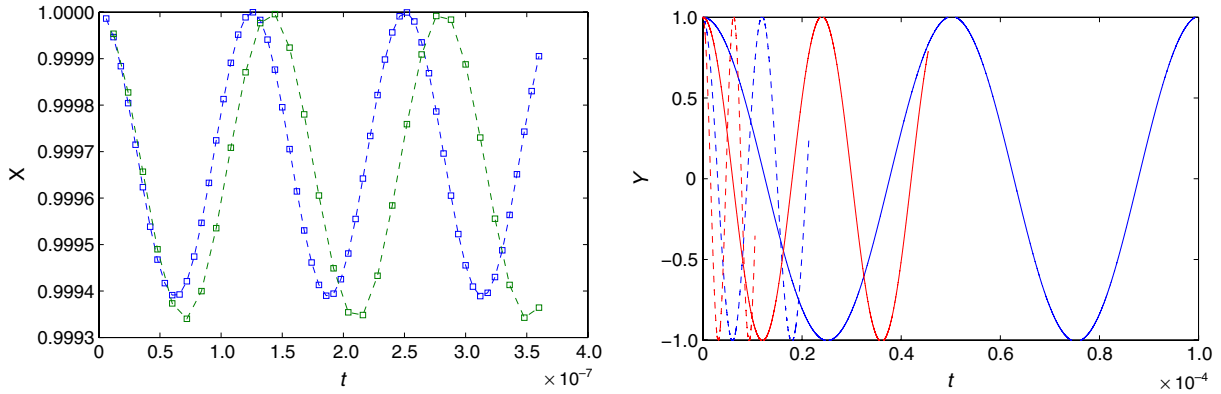


Figure 3. (a) $X = |\langle n | \otimes \langle - | V(t) | - \rangle \otimes | n \rangle|$ versus t for $(N, n) = (1, 2)$ (blue) and $(2, 2)$ (green), with $g = 10^8 \text{ s}(-1)$, $5\Theta = gN^{1/3}$, $\Omega = 100g$, and $\Delta_1 = 10\sqrt{N}g$; (b) $Y = \text{Re}(\langle n | \otimes \langle - | V(t) | - \rangle \otimes | n \rangle)$ versus t for $(N, n) = (1, 1)$ (blue solid line), $(1, 2)$ (blue dashed line), $(2, 1)$ (red solid line) and $(2, 2)$ (red dashed line), with $g = 10^8 \text{ s}^{-1}$, $\Delta_1 = 10g$, $\Theta = g$, and $\Omega = 100g$.

figure 3(a) we get a good agreement with the ideal case both for 1 and 2 atoms. In particular the quality of the approximation does not deteriorate with the number of atoms, as expected from our analytical calculations. In figure 3(b) in turn we plotted $\text{Re}(\langle n | \otimes \langle - | V(t) | - \rangle \otimes | n \rangle)$ for $(N, n) = (1, 1)$, $(1, 2)$, $(2, 1)$, $(2, 2)$, with the parameters $g = 10^8 \text{ s}^{-1}$, $\Delta_1 = 10g$, $\Theta = g$, and $\Omega = 100g$. We found a very good agreement with the dynamics of a pure photonic nonlinearity of strength $\kappa = Ng^4/4\Delta_1^2\Theta$, for which $\text{Re}(\langle n | \otimes \langle - | V(t) | - \rangle \otimes | n \rangle) = \cos(\kappa n^2 t)$.

The main source of decoherence in the system under analysis is spontaneous emission from the upper level and cavity decay due to the finite quality factor of the cavity used. Dephasing can usually be disregarded as its effects are much smaller. The upper level is hardly populated, so spontaneous emission from it should not play an important role. Indeed, the effective spontaneous emission rate can be estimated by the product of the population of the upper level $|2\rangle$, given by (g^2/Δ_1^2) , with the spontaneous emission rate. As we work in the regime $g/\Delta_1 \ll 1$, the effective spontaneous emission rate can be shown to be several orders of magnitude smaller than the effective nonlinearity (see section 6 for further discussion). The main source of decoherence is therefore cavity decay. First, as mentioned before, in order to justify the use of one single mode describing the cavity field, one needs to ensure that $\Delta_1, \Delta_2 \gg \kappa$, where κ is the cavity decay rate. The derivation can then be carried through independently of the exact value of κ . Of course in the end the dynamics will have a contribution from the effective nonlinear term and from the leaking out of photons from the cavity. In order to have a good approximation for a pure photonic nonlinearity the strength of the effective interaction should therefore be much larger than κ . As shown in section 6 this condition can indeed be achieved in several cavity QED set-ups.

We have numerically checked the effect of decoherence by simulating the full evolution in the case of one atom, considering the effect of dephasing, spontaneous emission from the upper level and cavity decay. The parameters used are $g = 10^9 \text{ s}^{-1}$, $\Lambda = 2g$, $\Delta_1 = 10\Lambda$, and $\Delta_2 = 5\Lambda$. Moreover, we consider $\kappa = 10^6 \text{ s}^{-1}$, $\gamma = 10^6 \text{ s}^{-1}$, and $\theta = 10^3 \text{ s}^{-1}$ for the cavity decay rate, spontaneous emission rate, and dephasing rate, respectively. As discussed in section 6, these parameters are within reach in several cavity QEP set-ups. The dynamics of

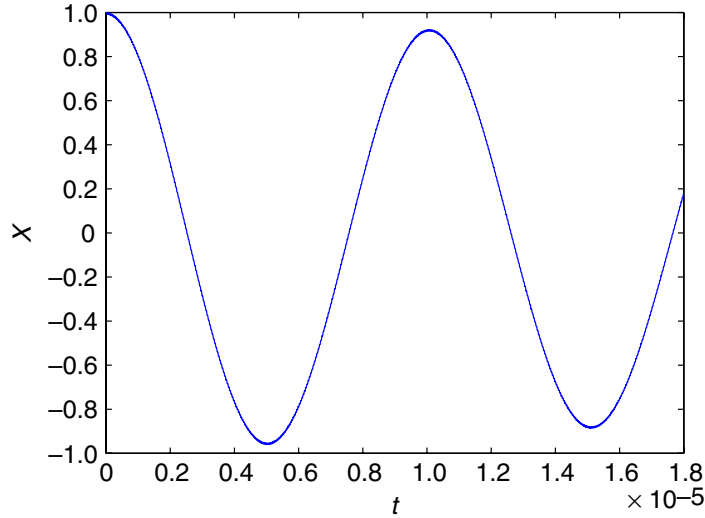


Figure 4. $X = \text{Re}(\langle 3| \otimes \langle -|V'(t)|- \rangle \otimes |1_k\rangle 3)$ versus t for $g = 10^9 \text{ s}^{-1}$, $\Lambda = 2g\Delta_1 = 10\Lambda$, $\Delta_2 = 5\Lambda$, $\kappa = 10^6 \text{ s}^{-1}$, $\gamma = 10^6 \text{ s}^{-1}$, and $\theta = 10^3 \text{ s}^{-1}$. The damping in the oscillations show the effect of losses due to spontaneous emission from the excited level, cavity decay rate, and dephasing from all three levels. With the realistic parameters considered one achieves a good approximation to the ideal case.

$\text{Re}(\langle 3| \otimes \langle -|V'(t)|- \rangle \otimes |3\rangle)$ is plotted in figure 4 where now $V'(t)$ is the non-unitary operator describing the full Hamiltonian and the decoherence sources. It should be contrasted with the evolution due to an ideal Kerr nonlinearity, given by $\cos(\kappa 9t)$.

5. Cross-Kerr nonlinearities

Up to now we have discussed the case of self-Kerr nonlinearities. In a cross-Kerr nonlinearity, one optical field induces a Stark shift in another field proportional to the intensity of the former. In terms of two optical modes a and b , the Hamiltonian is given by $H_{\text{cross}} = \nu a^\dagger a b^\dagger b$. There are two possible generalizations of the scheme introduced here to produce large cross-Kerr nonlinearities.

As shown in figure 5(a), we may choose settings as in equation (4), but now, we have a second cavity mode b coupled to the transition $|1\rangle \rightarrow |2\rangle$ with Rabi frequency g_b and detuning Δ_{1_b} . As shown in [32], this could be achieved using two degenerate cavity modes with orthogonal polarization. Carrying over the same analysis we did for the one mode case, we can find in this case

$$H_{\text{eff}} = \frac{1}{\Theta} \left(\frac{g_a^2}{2\Delta_{1_a}} a^\dagger a - \frac{g_b^2}{2\Delta_{1_b}} b^\dagger b \right)^2 S_3. \quad (17)$$

Hence, in addition to a self-Kerr nonlinearity for each mode, we find a cross-Kerr nonlinearity between them.

In the second case, we consider the level structure shown in figure 5(b). We have two modes a and b coupled to the transition $|0\rangle \rightarrow |2\rangle$ with detunings $\Delta_1 \pm \delta$, respectively. As discussed

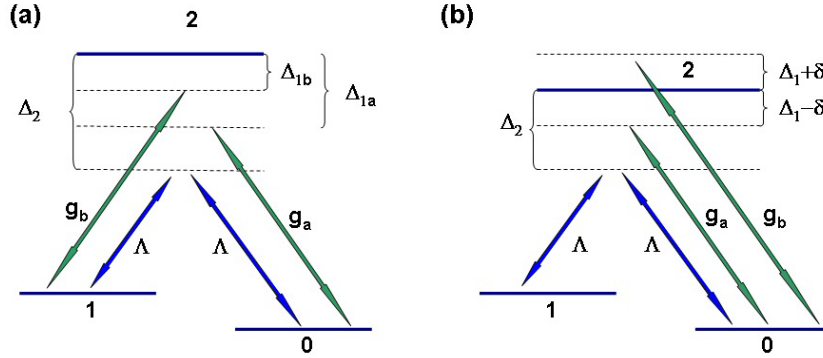


Figure 5. Level structures for generating cross-Kerr nonlinearities. Coupling to the cavity mode is shown in green and to classical lasers in blue.

in [25], this set-up could be realized in a toroidal microcavity, where a and b are the normal modes of the clockwise and counter-clockwise propagating modes, and δ is the rate of tunnelling between those two. In this case, the effective Hamiltonian can be found to be

$$H_{\text{eff}} = \frac{1}{\Theta} \left(\frac{g_a^2}{2(\Delta_1 - \delta)} a^\dagger a + \frac{g_b^2}{2(\Delta_1 + \delta)} b^\dagger b \right)^2 S_3. \quad (18)$$

6. Possible experimental realizations

Our scheme can be applied to a variety of cavity QED settings. This includes single or an ensemble of atoms trapped in fibre-based cavities [23] or optical microcavities [12], [24]–[27], where for the single atom case ratios of $\xi/\kappa \approx 625$ and $\xi/\gamma \approx 245$ for the nonlinearity strength (ξ) over cavity decay rate κ and effective spontaneous emission γ , respectively, have been predicted to be feasible [33], and quantum dots embedded in photonic bandgap structures, where ratios of $\xi/\kappa \approx 40$ and $\xi/\gamma \approx 12$ could be achieved [28]. Cooper-pair boxes coupled to a rf transmission line [29] could also be a suitable set-up in the longer run, when the problem related to the absence of two metastable levels is overcome. Even considering the decay between levels $|1\rangle$ and $|0\rangle$ in such systems, promising ratios of $\xi/\kappa \approx 15$ and $\xi/\gamma \approx 0.5$ could be realized [30] using the values of the recent experiment [30].

In implementations based on atoms, e.g. [2, 5, 12], [23]–[27], one can safely neglect the spontaneous emission from the two metastable levels, as their lifetime is several orders of magnitude larger than the time the photon stays in the cavity. In settings based on quantum dots, one can also find metastable configurations, whose lifetimes, although much smaller than in the atomic case, would still be large in comparison to the timescales involved in the experiment (see e.g. [34]). In such cases, the effective spontaneous emission rate is given by the product of the population of the upper level $|2\rangle$, given by g^2/Δ_1^2 , with the spontaneous emission rate. In the absence of two metastable levels, as it is the present case of rf cavities interacting with Cooper pair-boxes, γ is just the spontaneous emission rate from $|1\rangle$ to the ground state $|0\rangle$.

As an example of the applicability of our scheme to engineer nonlinearities which grow with the number of atoms, we consider the recent experiment [24] (see also [23]) in which a Bose–Einstein condensate of 4×10^5 ^{87}Rb atoms was strongly coupled to a single cavity mode

of an ultra-high finesse optical cavity, with cavity decay rate κ , spontaneous emission rate γ' and Rabi frequency g of 8, 18 and 70 MHz, respectively. We could apply our scheme to this set-up using for instance two Zeeman sublevels as the two metastable levels. The estimated nonlinearity ξ could then be as large as g itself, which would allow the realization of ratios $\xi/\kappa \approx 11$ and $\xi/\gamma \approx 39$ for nonlinearity strength (ξ) over cavity decay rate κ and spontaneous emission rate γ .

7. Summary

We have presented a new proposal for producing giant Kerr nonlinearities in cavity QED systems which generates nonlinearities at least two orders of magnitude larger than previously considered possible. These, in turn, could be applied to the implementation of photonic quantum information processing, as well as paving a way to the observation of quantum many-body phenomena in arrays of coupled cavities.

Acknowledgments

This work is part of the QIP-IRC supported by EPSRC (GR/1582176/01), the EU integrated project QAP supported by the IST directorate under contract no. 015848 and was supported by EPSRC (EP/E058256/1), the Brazilian agency CNPq, a Royal Society Wolfson Research Merit Award, and the Alexander von Humboldt Foundation.

Appendix. Derivation of the effective dynamics

In this appendix we provide a more explicit derivation of the effective Hamiltonian given by equation (10) in the hope of giving the reader a better understanding of the steps taken. To analyse the system Hamiltonian given by equation (4) more carefully, let us perform an adiabatic elimination of the upper atomic level, for the case of one atom in the sake of clarity. We first consider Dyson's series for the propagator of Hamiltonian (4) up to third order,

$$U(t, 0) \approx \mathbb{1} - i \int_0^t H(t_1) dt_1 - \int_0^t \int_0^{t_1} H(t_1) H(t_2) dt_1 dt_2 + i \int_0^t \int_0^{t_1} \int_0^{t_2} H(t_1) H(t_2) H(t_3) dt_1 dt_2 dt_3. \quad (\text{A.1})$$

We have

$$\int_0^t H(r) dr = \frac{igt}{\Delta_1} ((e^{-i\Delta_1 t} - 1)|0\rangle\langle 2|a^\dagger - (e^{i\Delta_1 t} - 1)|2\rangle\langle 0|a) + \frac{\sqrt{2}i\Lambda t}{\Delta_2} ((e^{-i\Delta_2 t} - 1)|+\rangle\langle 2| - (e^{i\Delta_2 t} - 1)|2\rangle\langle +|), \quad (\text{A.2})$$

and

$$\begin{aligned}
\int_0^t H(r) dr \int_0^r H(r') dr' = & \frac{ig^2}{\Delta_1} \left(-t|0\rangle\langle 0|a^\dagger a + \frac{ie^{-i\Delta_1 t}}{\Delta_1} |0\rangle\langle 0|a^\dagger a \right) \\
& + \frac{i\sqrt{2}\Lambda g}{\Delta_2} \left(-\frac{ie^{-i(\Delta_1-\Delta_2)t}}{\Delta_1-\Delta_2} |0\rangle\langle +|a^\dagger + \frac{ie^{-i\Delta_1 t}}{\Delta_1} |0\rangle\langle +|a^\dagger \right) \\
& + \frac{ig^2}{\Delta_1} \left(t|2\rangle\langle 2|aa^\dagger + \frac{ie^{i\Delta_1 t}}{\Delta_1} |2\rangle\langle 2|aa^\dagger \right) \\
& + \frac{i\sqrt{2}\Lambda g}{\Delta_1} \left(\frac{ie^{-i(\Delta_2-\Delta_1)t}}{\sqrt{2}(\Delta_2-\Delta_1)} |2\rangle\langle 2|a + \frac{ie^{i\Delta_1 t}}{\sqrt{2}\Delta_1} |2\rangle\langle 2|a \right) \\
& + \frac{i\sqrt{2}\Lambda g}{\Delta_1} \left(\frac{ie^{i(\Delta_1-\Delta_2)t}}{\Delta_1-\Delta_2} |+\rangle\langle 0|a + \frac{ie^{-i\Delta_2 t}}{\Delta_2} |+\rangle\langle 0|a \right) \\
& + \frac{i2\Lambda^2}{\Delta_2} \left(-t|+\rangle\langle +| + \frac{ie^{-i\Delta_2 t}}{\Delta_2} |+\rangle\langle +| \right) \\
& + \frac{ig\Lambda}{\Delta_1} \left(\frac{ie^{-i(\Delta_1-\Delta_2)t}}{\Delta_1-\Delta_2} |2\rangle\langle 2|a^\dagger - \frac{ie^{i\Delta_2 t}}{\Delta_2} |2\rangle\langle 2|a^\dagger \right) \\
& + \frac{i2\Lambda^2}{\Delta_2} \left(t|2\rangle\langle 2| + \frac{ie^{i\Delta_2 t}}{\Delta_2} |2\rangle\langle 2| \right). \tag{A.3}
\end{aligned}$$

The regime we are interested in, as outlined in the main text, is characterized by the following conditions:

$$g \ll \Delta_1, \quad \Lambda \ll \Delta_2, \tag{A.4}$$

$$\frac{\Lambda^3}{(\Delta_2)^2} \ll \frac{g^2}{\Delta_1} \ll \frac{\Lambda^2}{\Delta_2}. \tag{A.5}$$

There are two terms in the third-order term of Dyson's series which might be comparable to g^2/Δ_1 . Keeping just these, we have

$$\int_0^t H(r) dr \int_0^r H(r') dr' \int_0^{r'} H(r'') dr'' \approx \frac{t\sqrt{2}\Lambda^2 g}{\Delta_1 \Delta_2} |+\rangle\langle 2|a^\dagger - \frac{2t\Lambda^2 g}{\Delta_1 \Delta_2} |2\rangle\langle 0|a.$$

Hence,

$$\begin{aligned}
U(t, 0) \approx & \mathbb{1} + \frac{ig^2 t}{\Delta_1} |0\rangle\langle 0|a^\dagger a - \frac{ig^2 t}{\Delta_1} |2\rangle\langle 2|aa^\dagger + \frac{i2\Lambda^2 t}{\Delta_2} |+\rangle\langle +| - \frac{i2\Lambda^2 t}{\Delta_2} |2\rangle\langle 2| \\
& + \frac{it\sqrt{2}\Lambda^2 g}{\Delta_1 \Delta_2} |+\rangle\langle 2|a^\dagger - \frac{i2t\Lambda^2 g}{\Delta_1 \Delta_2} |2\rangle\langle 0|a. \tag{A.6}
\end{aligned}$$

Thus, we can approximate the propagator as follows

$$\begin{aligned}
U(t, 0) \approx & \exp \left(-it \left(\frac{g^2}{\Delta_1} |0\rangle\langle 0|a^\dagger a - \frac{g^2}{\Delta_1} |2\rangle\langle 2|aa^\dagger + \frac{2\Lambda^2}{\Delta_2} |+\rangle\langle +| \right. \right. \\
& \left. \left. - \frac{2\Lambda^2}{\Delta_2} |2\rangle\langle 2| + \frac{\sqrt{2}\Lambda^2 g}{\Delta_1 \Delta_2} |+\rangle\langle 2|a^\dagger - \frac{2\Lambda^2 g}{\Delta_1 \Delta_2} |2\rangle\langle 0|a \right) \right). \tag{A.7}
\end{aligned}$$

Defining

$$H := \frac{g^2}{\Delta_1} |0\rangle\langle 0| a^\dagger a - \frac{g^2}{\Delta_1} |2\rangle\langle 2| a a^\dagger + \frac{2\Lambda^2}{\Delta_2} |+\rangle\langle +| - \frac{2\Lambda^2}{\Delta_2} |2\rangle\langle 2| + \frac{\sqrt{2}\Lambda^2 g}{\Delta_1 \Delta_2} |+\rangle\langle 2| a^\dagger - \frac{2\Lambda^2 g}{\Delta_1 \Delta_2} |2\rangle\langle 0| a, \quad (\text{A.8})$$

we can go to the interaction picture with respect to

$$\frac{2\Lambda^2}{\Delta_2} |+\rangle\langle +| - \left(\frac{2\Lambda^2}{\Delta_2} - \frac{g^2}{\Delta_1} \right) |2\rangle\langle 2| + \frac{g^2}{2\Delta_1} a^\dagger a \quad (\text{A.9})$$

and obtain an effective Hamiltonian, which—up to unimportant constants—is given by:

$$\frac{g^4}{\Delta_1^2 \Theta} (S_{01} + S_{10}) (a^\dagger a)^2 + \lambda |+\rangle\langle +| a^\dagger a + \mu |2\rangle\langle 2| a^\dagger a a^\dagger a \quad (\text{A.10})$$

where μ and ν are of the same order as $(g^4/\Delta_1^2 \Theta)$. If we now prepare the atom into the state $|-\rangle$, we get only the desired Kerr nonlinear term given by equation (10).

References

- [1] Walls D F and Milburn G J 1994 *Quantum Optics* (Berlin: Springer)
- [2] Raimond J M, Brune M and Haroche S 2001 *Rev. Mod. Phys.* **73** 565
- [3] Imoto N, Haus H A and Yamamoto Y 1985 *Phys. Rev. A* **32** 2287
- [4] Fleischhauer M and Lukin M D 2002 *Phys. Rev. A* **65** 022314
- [5] Turchette Q A, Hood C J, Lange W, Mabuchi H and Kimble H J 1995 *Phys. Rev. Lett.* **75** 4710
- [6] Mabuchi H and Doherty A C 2002 *Science* **298** 1372
- [7] Imamoğlu A, Schmidt H, Woods G and Deutsch M 1997 *Phys. Rev. Lett.* **79** 1467
Imamoğlu A, Schmidt H, Woods G and Deutsch M 1998 *Phys. Rev. Lett.* **81** 2836
Werner M J and Imamoğlu A 1999 *Phys. Rev. A* **61** 011801
- [8] Hartmann M J and Plenio M B 2007 *Phys. Rev. Lett.* **99** 103601
- [9] Hartmann M J, Brandão F G S L and Plenio M B 2006 *Nat. Phys.* **2** 849
- [10] Fleischhauer M, Imamoğlu A and Marangos J P 2005 *Rev. Mod. Phys.* **77** 633
- [11] Hau L V, Harris S E, Dutton Z and Behroozi C H 1999 *Nature* **397** 594
- [12] Birnbaum K M, Boca A, Miller R, Boozer A D, Northup T E and Kimble H J 2005 *Nature* **436** 87
- [13] Angelakis D G, Santos M F and Bose S 2007 *Phys. Rev. A* **76** 031805
- [14] Greentree A D, Tahan C, Cole J H and Hollenberg L C L 2006 *Nat. Phys.* **2** 856
- [15] Neil Na Y C, Utsunomiya S, Tian L and Yamamoto Y 2007 *Preprint* quant-ph/0703219v4
- [16] Irish E K, Ogden C D and Kim M S 2007 *Preprint* 0707.1497
- [17] Rossini D and Fazio R 2007 *Phys. Rev. Lett.* **99** 186401
- [18] Hartmann M J, Brando F G S L and Plenio M B 2007 *Phys. Rev. Lett.* **99** 160501
- [19] Hartmann M J and Plenio M B 2007 *Preprint* 0708.2667
- [20] Munro W J, Nemoto K, Beausoleil R G and Spiller T P 2005 *Phys. Rev. A* **71** 033819
- [21] Nemoto K and Munro W J 2004 *Phys. Rev. Lett.* **93** 250502
- [22] Duan L M, Giedke G, Cirac J I and Zoller P 2000 *Phys. Rev. Lett.* **84** 4002
Duan L M, Giedke G, Cirac J I and Zoller P 2000 *Phys. Rev. A* **62** 032304
- [23] Colombe Y, Steinmetz T, Dubois G, Linke F, Hunger D and Reichel J 2007 *Nature* **450** 272
- [24] Brennecke F, Donner T, Ritter S, Bourdel T, Köhl M and Esslinger T 2007 *Nature* **450** 268
- [25] Aoki T, Dayan B, Wilcut E, Bowen W P, Parkins A S, Kippenberg T J, Vahala K J and Kimble H J 2006 *Nature* **443** 671
Armani D K, Kippenberg T J, Spillane S M and Vahala K J 2003 *Nature* **421** 925

- [26] Trupke M, Hinds E A, Eriksson S, Curtis E A, Muktadir Z, Kukhareuka E and Kraft M 2005 *Appl. Phys. Lett.* **87** 211106
- [27] Hijlkema M, Weber B, Specht H P, Webster S C, Kuhn A and Rempe G 2007 *Nat. Phys.* **3** 253
- [28] Hennessy K, Badolato A, Winger M, Gerace D, Atatüre M, Gulde S, Fält S, Hu E L and Imamoglu A 2007 *Nature* **445** 896
- [29] Ahkane Y, Asano T and Song B S 2003 *Nature* **425** 944
- [29] Wallraff A, Schuster D I, Blais A, Frunzio L, Huang R-S, Majer J, Kumar S, Girvin S M and Schoelkopf R J 2004 *Nature* **431** 162
- [30] Schuster D I *et al* *Nature* **445** 515
- [31] Klimov A B and Sanchez-Soto L L 2000 *Phys. Rev. A* **61** 063802
- [32] Duan L-M and Kimble H J 2003 *Phys. Rev. Lett.* **90** 253601
- [33] Spillane S M, Kippenberg T J, Vahala K J, Goh K W, Wilcut E and Kimble H J 2005 *Phys. Rev. A* **71** 013817
- [34] Türeci H E, Taylor J M and Imamoglu A 2006 *Preprint cond-mat/0611469*